Research paper

Synergistic Control of Permeability and Selectivity in Nanofiltration Membranes through UiO-66/Graphene Oxide Hybrid Fillers

Muhammad Ammar Farooq[a], Noaman Ul Haq[a,*], Ghulam Muhammad[b], Hira Naveed[c]

[a] Department of Chemical Engineering, COMSATS University Islamabad, Lahore Campus, Pakistan
[b] Chemical Engineering Program, Graduate School of Advanced Science and Engineering, Hiroshima University, Higashi-Hiroshima, 739-8527, Japan
[c] School of Civil Engineering and Environmental Science, University of Oklahoma, Norman, OK, USA

* *Corresponding author:* noamanulhaq@cuilahore.edu.pk

Abstract: The selective removal of toxic heavy metals from water remains a critical challenge for nanofiltration membranes due to the inherent permeability–selectivity trade-off. Herein, thin film nanocomposite (TFN) nanofiltration membranes incorporating zirconium-based metal organic framework UiO-66, graphene oxide (GO), and UiO-66/GO hybrid fillers were fabricated via interfacial polymerization on polyacrylonitrile supports. Structural and chemical characterization confirmed preservation of UiO-66 crystallinity and polyamide selective layer integrity, while GO hybridization significantly improved filler dispersion and interfacial compatibility. Membrane performance evaluation demonstrated that filler morphology and hybrid architecture strongly influence transport and separation behavior. The optimized TFN membrane incorporating UiO-66/GO hybrid fillers achieved a high Cr(VI) rejection exceeding 95% along with a water permeability of approximately 12 LMH bar^{-1}, representing more than a twofold improvement compared to the pristine membrane while maintaining high selectivity. The preferential rejection of potassium dichromate relative to NaCl confirms dominant Donnan electrostatic exclusion reinforced by filler-regulated transport pathways. Surface wettability analysis further revealed that hybrid fillers enable controlled hydrophilicity without compromising membrane integrity or stability. These findings demonstrate that UiO-66/GO hybrid fillers effectively mitigate the permeability–selectivity trade-off and provide a scalable strategy for developing high-performance nanofiltration membranes for selective removal of toxic multivalent contaminants from water.

Keyword: Nanofiltration membranes; Thin film nanocomposite membranes; Metal organic frameworks; Chromium removal; Water treatment

1. Introduction

Global drinking water scarcity has emerged as one of the most pressing challenges to sustainable development, driven not only by population growth and climate variability but increasingly by the deterioration of water quality due to industrial contamination [1, 2]. A substantial fraction of freshwater resources worldwide is rendered unsuitable for human consumption as a result of heavy metal pollution originating from electroplating, leather tanning, textile dyeing, metal finishing, and chromite processing industries [3, 4]. Among these contaminants, chromium is of particular concern because of its high environmental mobility and the severe toxicity of its hexavalent form, Cr(VI), which is carcinogenic, mutagenic, and persistent even at trace concentrations [5, 6]. Conventional chromium removal technologies, including chemical precipitation, adsorption, coagulation–flocculation, and ion exchange, have demonstrated effectiveness under controlled laboratory conditions. However, their large-scale deployment is frequently hindered by high chemical consumption, secondary sludge generation, sensitivity to pH and competing ions, and rising operational and disposal costs [7, 8]. Membrane technology is recognized as one of the most sustainable separation technologies for both gas and liquid systems due to its low energy consumption, minimal environmental footprint, and cost-effectiveness [9–11]. Nanofiltration (NF) based membrane processes offer a favorable balance between separation efficiency and energy demand for heavy metals removal. NF membranes are capable of selectively rejecting multivalent ions and chromate species at significantly lower operating pressures than reverse osmosis, while maintaining higher water permeability and modular scalability [12, 13].

Received 7 January 2026, Revised 6 February 2026, Accepted 8 February 2026, Available online 18 February 2026

Despite these advantages, issues related to fouling, long-term chemical stability, and the intrinsic permeability–selectivity trade-off continue to restrict widespread commercialization. There is a need for advanced NF membrane structures that combine selective ion transport, adsorption functionality, and structural robustness for effective chromium removal from contaminated water streams [14, 15].

NF membranes used in water treatment have traditionally been dominated by thin film composite membranes (TFC) prepared by interfacial polymerization, owing to their low production cost, ease of processing, and scalability for industrial deployment [16, 17]. Despite their widespread use, polymeric membranes face inherent limitations that restrict their application in metal-contaminated and chemically aggressive wastewaters. These include poor resistance to extreme pH and oxidizing environments, susceptibility to fouling and compaction, limited control over pore size distribution, and an intrinsic permeability–selectivity trade-off, which constrains simultaneous enhancement of flux and ion rejection [2]. In contrast, inorganic membranes, such as ceramic, silica, and zeolitic membranes, offer superior thermal, mechanical, and chemical stability, making them attractive for harsh separation environments [18, 19]. However, their practical adoption remains limited due to high fabrication costs, brittleness, difficulty in producing defect-free ultrathin selective layers, and challenges associated with module integration and large-scale manufacturing [20, 21] To reconcile the processability of polymeric membranes with the robustness and selectivity of inorganic materials, thin film composite (TFN) membranes emerged as a promising nanofiltration architecture. TFN incorporate functional inorganic fillers, such as metal organic frameworks, zeolites, TiO2 or carbon-based nanomaterials, into polymer matrices, enabling synergistic enhancement of membrane performance through adsorption-assisted transport, improved hydrophilicity, and tailored ion–membrane interactions [22, 23]. By judicious selection and dispersion of fillers, TFN offer a viable pathway to overcome the longstanding limitations of both purely polymeric and purely inorganic membranes, particularly for the selective removal of multivalent heavy metal species from complex aqueous environments [24, 25].

MOFs have emerged as a superior class of fillers for TFN due to their exceptionally high surface area, tunable pore architecture, and chemically addressable metal–ligand coordination environments, which enable selective ion interactions beyond conventional size-based sieving mechanisms [22, 23]. Among the wide range of MOFs investigated for water treatment, zirconium-based UiO-66 has attracted particular interest owing to its outstanding hydrolytic stability, chemical resistance over a broad pH range, and robust $Zr_6O_4(OH)_4$ secondary building units, which remain structurally intact under conditions that degrade many other MOF families [26, 27]. Several studies have demonstrated that UiO-66 exhibits strong affinity toward oxyanionic and multivalent species, including chromate and dye molecules, through a combination of electrostatic interactions, coordination at unsaturated metal sites, and size-compatible pore confinement, making it particularly attractive for water purification applications [28, 29]. In parallel, graphene oxide (GO) has been extensively explored as a functional nanofiller in TFN due to its two-dimensional morphology, high aspect ratio, and abundance of oxygen-containing functional groups, which can improve membrane hydrophilicity, suppress fouling, and introduce additional transport pathways when properly dispersed [30, 31]. Prior studies on GO-based membranes have reported enhanced water flux and improved rejection of heavy metals and dyes; however, excessive GO loading often leads to nanosheet restacking, non-selective void formation, and permeability loss [32, 33]. The complementary characteristics of UiO-66 and GO enable the integration of selective adsorption and structural rigidity imparted by the MOF with the enhanced hydrophilicity and interfacial compatibility provided by GO. Together, these features create MMM architectures that offer a rational pathway to overcoming the individual limitations of each filler while enabling synergistic performance enhancements in nanofiltration-based water treatment.

In this work, we report a systematically engineered UiO-66/GO TFN to address persistent limitations of conventional asymmetric polymeric membranes for waste water treatment. Unlike prior studies that primarily treat MOFs or GO as independent permeability enhancers, the present approach exploits their complementary physicochemical roles to regulate ion–membrane interactions, transport pathways, and structural stability within a single membrane architecture. By optimizing filler loading and interfacial compatibility, this work demonstrates how selective rejection, water permeability, and membrane stability can be concurrently improved without sacrificing mechanical integrity or process scalability. These findings establish a clear structure–performance relationship for UiO-66/GO-based TFN and advance their rational design for nanofiltration applications, positioning this membrane architecture as a viable platform for efficient and robust removal of chromium species from complex aqueous environments.

2. Materials and Methods

2.1 Materials

Terephthalic acid (H_2BDC, ≥99%) and zirconium(IV) chloride ($ZrCl_4$, ≥99.5%) were used as organic linker and metal precursor, respectively, for the synthesis of the MOF. Polyacrylonitrile (PAN) served as the membrane forming polymer, while N-methyl-2-pyrrolidone (NMP, anhydrous) was employed as the solvent for membrane casting. Methanol (HPLC grade) was used for solvent exchange and washing steps. A non-woven polypropylene/polyethylene support fabric (Novatexx 2471) was kindly supplied by Freudenberg Filtration Technologies, Germany n. m-Phenylenediamine (MPD, ≥99%) and trimesoyl chloride (TMC, ≥99%) were used as aqueous and organic phase monomers, respectively, for interfacial polymerization, with n-hexane (≥95%) as the organic solvent. Sodium chloride (NaCl) and potassium dichromate ($K_2Cr_2O_7$) were used as model salts for membrane performance evaluation. Triethylamine (TEA, ≥99%) and sodium dodecyl sulfate (SDS, aqueous solution) were used as additives where specified. All chemicals were used as received without further purification, and deionized water was used throughout all experiments.

2.2 Synthesis of UiO-66

UiO-66 was synthesized via a solvothermal method using zirconium(IV) chloride as the metal precursor and terephthalic acid (H_2BDC) as the organic linker. In a typical synthesis, 0.70 g of $ZrCl_4$ (3.0 mmol) and 0.50 g of H_2BDC (3.0 mmol) were dissolved in 50 mL of N,N-dimethylformamide (DMF) under magnetic stirring to obtain a homogeneous precursor solution. The mixture was sonicated for 10 min to ensure complete dissolution and subsequently transferred into a sealed Teflon-lined stainless-steel autoclave. Solvothermal crystallization was carried out at 80 °C for 24 h. After naturally cooling to room temperature, the resulting white precipitate was recovered by centrifugation and washed three times with fresh DMF to remove unreacted species and residual linker. Solvent exchange was then performed by dispersing the solid in methanol for 24 h, with methanol refreshed every 8 h. The product was finally dried in an oven at 80 °C for 24 h to obtain a free-flowing UiO-66 powder, which was gently ground using a mortar and pestle and stored in airtight containers for subsequent use.

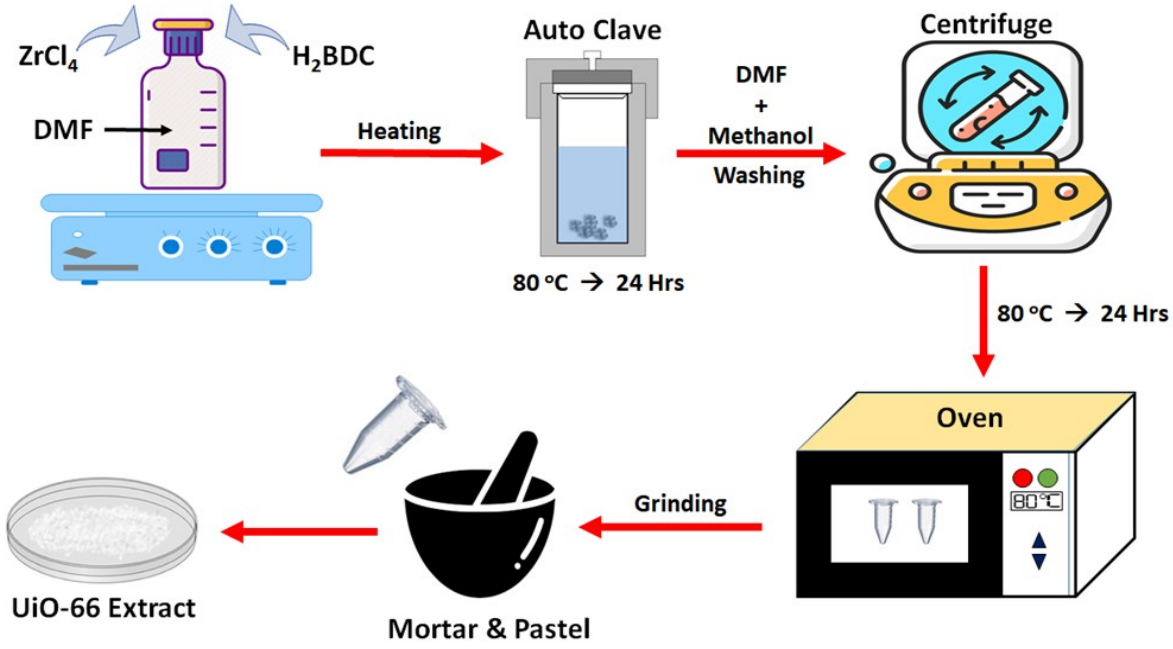

Figure 1. Schematic illustration of the solvothermal synthesis and post-treatment of UiO-66

2.3 Synthesis of UiO-66/GO Composite

UiO-66/GO composites were prepared by physically integrating UiO-66 with GO at different weight ratios. In a typical preparation, 0.20 g of UiO-66 was combined with GO at 10, 20, and 30 wt% relative to the mass of UiO-66. The required amount of GO was dispersed in methanol and mixed with UiO-66 under continuous shaking to ensure uniform distribution. The resulting suspension was centrifuged at 8000 rpm for 10 min, and the supernatant was discarded. The collected solid was then dried in an oven at 80 °C for 24 h to remove residual solvent and moisture. After drying, the composite was gently ground using a mortar and pestle to obtain a homogeneous fine powder. The resulting UiO-66/GO composite powders were stored in airtight vials for subsequent membrane fabrication.

2.4 Fabrication of PAN Support Membranes

Asymmetric PAN supports were prepared via phase inversion. A 16 wt% PAN casting solution was formulated by dissolving PAN in NMP at a PAN:NMP mass ratio of 16:84, yielding a total solution mass of 50 g. The mixture was stirred continuously for 24 h at room temperature to obtain a homogeneous dope solution and then degassed prior to casting. The solution was cast onto a nonwoven fabric using a membrane casting machine (Elcometer, UK) to ensure uniform film formation. Immediately after casting, the film was immersed in a deionized (DI) water coagulation bath for 10 min to induce phase inversion. The resulting porous PAN supports were stored in DI water until further use.

2.5 Fabrication of TFC and TFN Membranes

TFC and TFN membranes were fabricated via interfacial polymerization on PAN supports. The wet PAN support was immersed in 2 wt% MPD aqueous solution for 4 min to allow monomer uptake. Excess solution was removed using a rubber roller, and the support was fixed in an acrylic frame exposing only the active surface. Interfacial polymerization was initiated by contacting the surface with 0.2 wt% TMC/n-hexane solution, containing dispersed nanofillers where applicable, for 60 s. During this process, the nanofillers became physically embedded and immobilized within the forming polyamide selective layer. This encapsulation within the dense crosslinked polyamide network enhances filler retention and minimizes potential leaching during operation. The formed polyamide layer was thermally cured at 50 °C for 10 min in an oven to promote structural stability and interfacial integrity. Finally, the membranes were thoroughly rinsed and stored in DI water at room temperature prior to characterization. TFC membranes were prepared using filler-free organic solution, while TFN membranes incorporated UiO-66, GO, or UiO-66/GO composites at specified loadings to ensure uniform dispersion and stable incorporation within the selective layer.

Table 1. Tables should be placed in the main text near to the first time they are cited.

Membrane Code	Membrane Type	Filler Loading (wt%)
TFC-0	TFC (Control)	0.00
TFN-U-0.01	TFN	0.01
TFN-U-0.05	TFN	0.05
TFN-U-0.15	TFN	0.15

2.6 Characterization techniques

The morphology of the synthesized UiO-66 and UiO-66/GO composite powders was examined using scanning electron microscopy (SEM) to assess particle morphology. Prior to imaging, the samples were coated with a thin conductive gold layer to minimize surface charging during analysis. Fourier transform infrared (FTIR) spectroscopy was employed to identify functional groups and to verify chemical interactions in the PAN supports, UiO-66, UiO-66/GO composites, and composite membranes. FTIR spectra were recorded using a PerkinElmer Spectrum Two spectrometer equipped with a horizontal attenuated total reflectance (HATR) accessory, over a scan range of 4000–1000 cm^{-1}. The crystalline structure and phase purity of UiO-66 and UiO-66/GO composites were examined by powder X-ray diffraction (XRD) using a Rigaku MiniFlex 600-C diffractometer with Cu Kα radiation (λ = 1.5406 Å) over a 2θ range of 5°–70° at a scan rate of 2° min^{-1}.

2.7 Membrane Performance Evaluation

The performance of the fabricated membranes was evaluated using a dead-end filtration cell (Sterlitech HP4750) operated under constant pressure. Circular membrane samples with an effective filtration area of 14.6 cm^2 were mounted in the cell, and all experiments were conducted at room temperature. Prior to testing, membranes were compacted using DI water at the operating pressure for 30 min to achieve a stable flux.

Pure water flux was measured using DI water as the feed. The permeate volume was recorded as a function of time under a fixed transmembrane pressure. The pure water flux (Jw) was calculated according to:

$$J_w = \frac{V}{A\,t} \tag{1}$$

where V is the volume of permeate collected (L), A is the effective membrane area (m^2), and t is the filtration time (h). The water permeability (Pw) was obtained by normalizing the flux with respect to applied pressure:

$$P_w = \frac{J_w}{\Delta P} \tag{2}$$

where ΔP is the applied transmembrane pressure (bar). Water permeability is reported in units of L m^{-2} h^{-1} bar^{-1} (LMH bar^{-1}).

Membrane separation performance was evaluated using sodium chloride (NaCl) and potassium dichromate ($K_2Cr_2O_7$) aqueous solutions as model monovalent and multivalent solutes, respectively. All feed solutions were prepared in deionized water and maintained at neutral pH conditions (pH 6.5–7.0) without further adjustment. Under this pH range, Cr(VI) predominantly exists as negatively charged chromate (CrO_4^{2-}) and dichromate ($Cr_2O_7^{2-}$) species. The feed solutions were filtered under identical operating conditions, and permeate samples were collected after steady-state flux was achieved. Solute concentrations in the feed (Cf) and permeate (Cp) were determined using appropriate analytical methods to calculate rejection performance.

The solute rejection (R) was calculated using the following equation:

$$R(\%) = \left(1 - \frac{C_p}{C_f}\right) \times 100 \tag{3}$$

where Cf and Cp represent the solute concentrations in the feed and permeate, respectively. All membrane samples, including the pristine TFC membrane and TFN membranes incorporating UiO-66, GO, or UiO-66/GO composite fillers at different loadings, were tested under identical conditions to ensure direct comparison. The influence of filler type and loading on pure water permeability, NaCl rejection, and chromate rejection was systematically evaluated. Each experiment was repeated at least three times, and average values were reported to ensure data reliability.

All membrane fabrication and performance measurements were conducted in repeated trials under identical conditions to ensure reproducibility. The observed permeability, rejection, and contact angle values were consistent across repeated measurements, confirming the reliability of the reported data.

3. Results and Discussion

3.1 Physicochemical Characterization of UiO-66 and UiO-66/GO Fillers

The crystalline structure and phase integrity of the synthesized UiO-66 and UiO-66/GO composites were examined by powder XRD, as shown in Figure 2. The diffraction pattern of pristine UiO-66 exhibits the characteristic reflections at low 2θ values,

which are consistent with the well-defined crystalline framework of UiO-66 reported in the literature [34]. These reflections confirm the successful formation of the UiO-66 structure without detectable secondary phases, indicating high phase purity of the synthesized MOF. Upon incorporation of GO to form the UiO-66/GO composite, the diffraction pattern largely preserves the characteristic UiO-66 reflections, suggesting that the crystalline framework of UiO-66 remains structurally intact after composite formation. The absence of any significant peak shift or disappearance indicates that the interaction between UiO-66 and GO does not disrupt the long-range crystallographic order of the MOF. Notably, no distinct diffraction peak corresponding to GO is observed in the composite pattern, which can be attributed to the low loading level of GO and its intrinsically disordered, exfoliated nature, as well as the dominant diffraction contribution from the crystalline UiO-66 phase.

A slight reduction in peak intensity is observed for the UiO-66/GO composite compared to pristine UiO-66, which is commonly associated with partial coverage of UiO-66 crystallites by GO nanosheets and increased scattering from the amorphous GO component. Importantly, the retention of UiO-66 crystallinity after composite formation is critical for ensuring that the intrinsic porosity and adsorption functionality of the MOF are preserved when incorporated as a filler into TFN membranes.

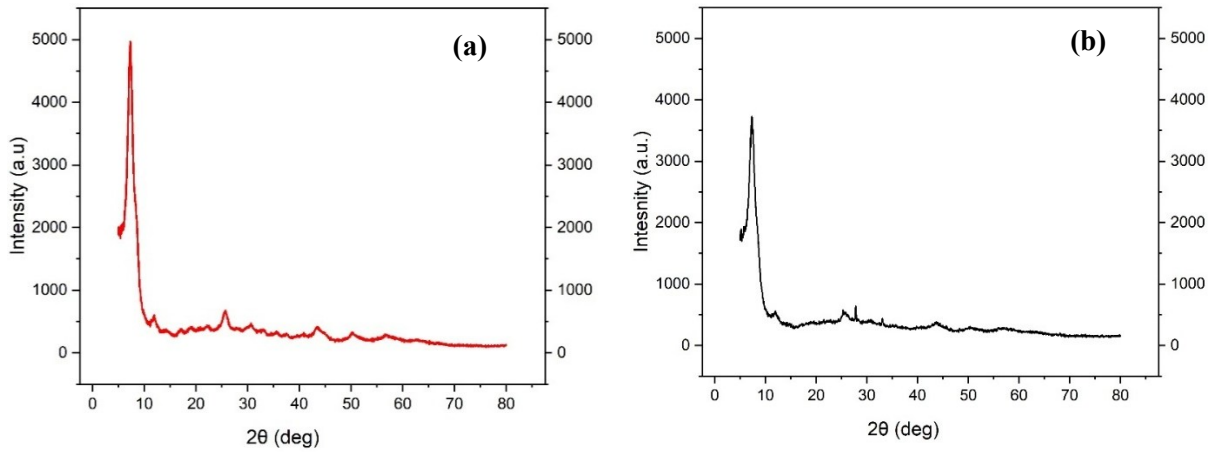

Figure 2. X-ray diffraction patterns of (a) UiO-66 and (b) UiO-66/GO composite fillers

FTIR spectroscopy was employed to probe the functional groups and interfacial interactions in UiO-66, GO, and the UiO-66/GO composite, as shown in Figure 3. The FTIR spectrum of pristine UiO-66 exhibits characteristic absorption bands associated with the terephthalate linker and Zr–O coordination environment. The broad band observed in the region of ~3200–3600 cm^{-1} is attributed to O–H stretching vibrations, arising from μ_3-OH groups within the $Zr_6O_4(OH)_4$ clusters as well as adsorbed moisture, which is typical for zirconium-based MOFs. Prominent bands in the range of ~1500–1600 cm^{-1} correspond to aromatic C=C stretching vibrations of the benzene ring in the terephthalate linker, while strong absorptions near ~1400–1550 cm^{-1} and ~1000–1200 cm^{-1} are assigned to symmetric and asymmetric stretching of the carboxylate (C–O) groups coordinated to Zr nodes.

The FTIR spectrum of GO displays characteristic features associated with oxygen-containing functional groups introduced during the oxidation of graphite. In particular, the absorption band around ~1000–1200 cm^{-1} is attributed to C–O stretching vibrations of epoxy and alkoxy groups, confirming the highly functionalized nature of GO. These surface oxygen functionalities are critical for promoting interfacial compatibility with UiO-66 and for enhancing dispersion within polymer matrices.

In the UiO-66/GO composite, the FTIR spectrum retains the key vibrational features of UiO-66, indicating that the fundamental coordination structure of the MOF remains intact after composite formation. Simultaneously, the presence and relative enhancement of C–O related bands suggest successful incorporation of GO within the composite. Notably, the absence of new covalent-bond-related peaks and the preservation of UiO-66 linker signatures indicate that the interaction between UiO-66 and GO is predominantly governed by non-covalent interactions, such as hydrogen bonding and electrostatic interactions, rather than framework alteration. This interaction mode is advantageous, as it preserves the intrinsic porosity and adsorption functionality of UiO-66 while utilizing the surface chemistry of GO to improve composite stability and interfacial compatibility.

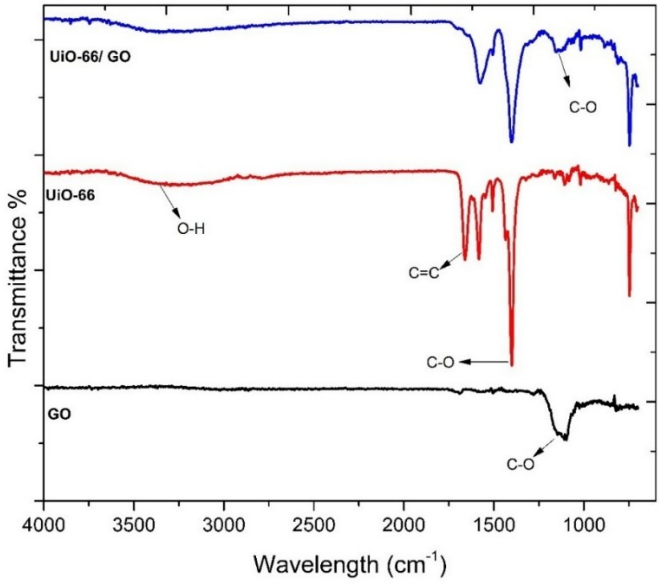

Figure 3. FTIR spectra of GO, pristine UiO-66, and UiO-66/GO composite fillers.

The morphological features of pristine UiO-66 and the UiO-66/GO composite fillers were examined using scanning electron microscopy, as shown in Figure 4. Pristine UiO-66 exhibits a relatively uniform population of well-defined polyhedral crystallites with sharp edges and faceted surfaces, which is characteristic of highly crystalline zirconium-based MOFs synthesized via solvothermal routes. The particles appear densely packed with a narrow size distribution, indicating controlled nucleation and growth during synthesis. Such well-developed crystal morphology is consistent with the preserved crystallinity observed in the XRD analysis and is favorable for maintaining accessible internal porosity.

In contrast, the UiO-66/GO composite displays a distinctly different morphological appearance. The particles appear partially embedded within or decorated by irregular, sheet-like structures attributed to graphene oxide. The composite morphology is more heterogeneous, with evidence of UiO-66 crystallites anchored onto or wrapped by GO sheets, leading to a rougher and less defined surface texture compared to pristine UiO-66. This morphological integration suggests intimate interfacial contact between UiO-66 and GO, which can be attributed to physical interactions such as hydrogen bonding and electrostatic attraction between the oxygenated functional groups of GO and the surface hydroxyl groups of UiO-66.

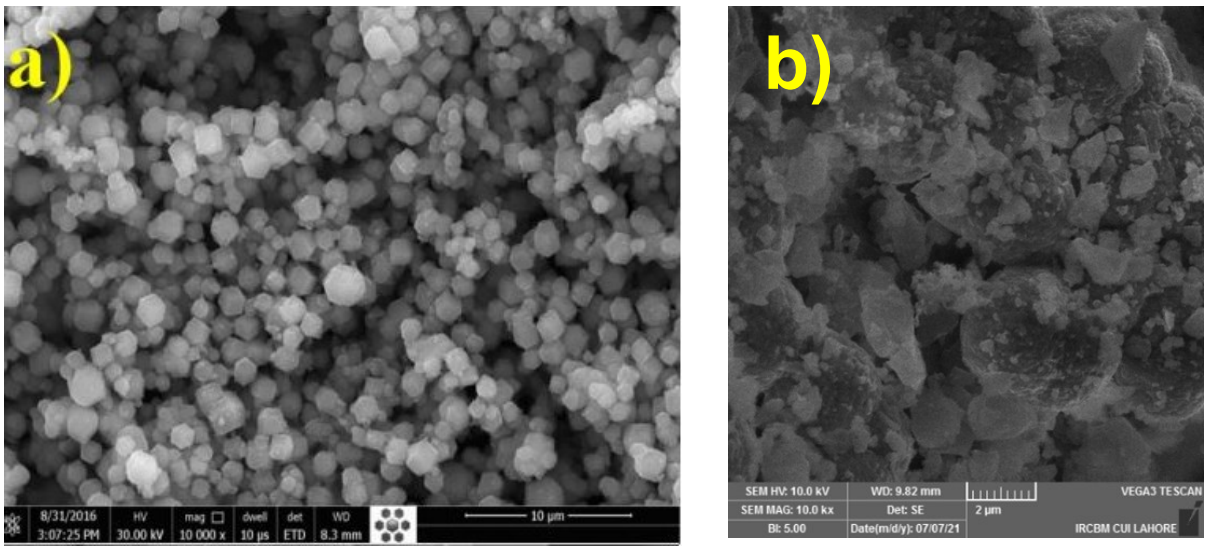

Figure 4. SEM images of (a) pristine UiO-66 and (b) UiO-66/GO composite fillers.

3.2 Characterization of TFC and TFN Membranes

The chemical structure of the pristine TFC membrane and TFN membranes incorporating UiO-66, GO, and UiO-66/GO composite fillers at different loadings was investigated using FTIR spectroscopy, as shown in Figure 5a and Figure 5b. The FTIR spectrum of the neat membrane exhibits characteristic absorption bands associated with the polyamide selective layer, including broad O–H/N–H stretching vibrations in the range of 3200–3500 cm^{-1}, C–H stretching vibrations near ~2900 cm^{-1}, and prominent amide I and amide II bands corresponding to C=O stretching and N–H bending vibrations in the region of ~1650–1550 cm^{-1}. These features confirm the successful formation of the polyamide layer via interfacial polymerization.

For UiO-66-based TFN membranes (Figure 5a), the overall spectral features remain largely consistent with those of the neat membrane, indicating that incorporation of UiO-66 does not alter the fundamental chemical structure of the polyamide matrix. However, a gradual increase in the intensity of carbonyl-related bands with increasing UiO-66 loading is observed, which can be attributed to the presence of carboxylate functionalities from the UiO-66 linker and enhanced hydrogen-bonding interactions between the MOF surface and the polyamide chains. Importantly, no new absorption bands corresponding to covalent bond formation are detected, suggesting that UiO-66 is physically embedded within the polyamide layer without disrupting the interfacial polymerization chemistry.

A similar trend is observed for GO-based TFN membranes and UiO-66/GO composite membranes (Figure 5b). The spectra display additional contributions in the region associated with oxygen-containing functional groups, particularly C–O stretching vibrations, which become more pronounced with increasing filler loading. These features are characteristic of GO and confirm its successful incorporation within the polyamide matrix. The preservation of the amide I and II bands across all membranes indicates that the polyamide network remains chemically intact, while the progressive enhancement of oxygenated functional group signals suggests increased interfacial interactions between the fillers and the polymer chains.

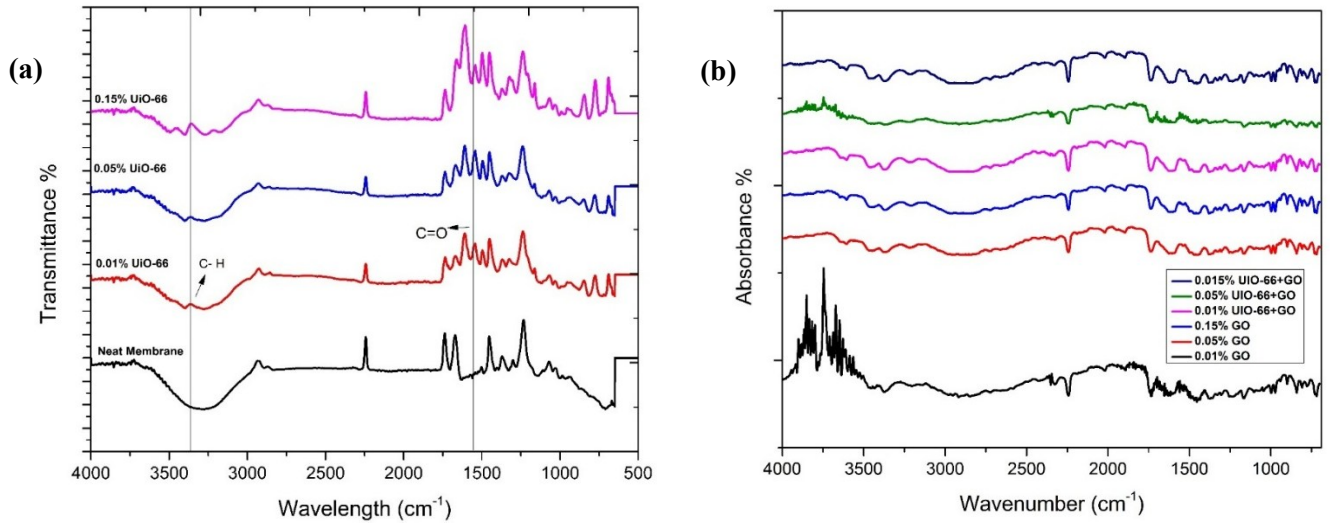

Figure 5. FTIR spectra of (a) UiO-66-based TFN membranes and (b) GO-based and UiO-66/GO composite TFN membranes at different filler loadings

Notably, the FTIR spectra of UiO-66/GO composite-based membranes exhibit features arising from both UiO-66 and GO without the appearance of new bands or peak shifts, indicating that the composite fillers are incorporated through non-covalent interactions rather than chemical modification of the polyamide layer. This interaction mode is desirable, as it preserves the intrinsic transport properties of the polyamide matrix while enabling modulation of surface chemistry and hydrophilicity through controlled filler loading. Overall, the FTIR results confirm the successful fabrication of chemically stable TFN membranes and provide evidence that UiO-66, GO, and UiO-66/GO fillers are incorporated without compromising the integrity of the selective polyamide layer.

The surface wettability of the pristine polyamide membrane and TFN membranes incorporating UiO-66, GO, and UiO-66/GO composite fillers at different loadings was evaluated through static water contact angle measurements, as shown in Figure 6. The neat polyamide membrane exhibits a moderate contact angle of approximately 40°, indicating an intrinsically hydrophilic surface consistent with the presence of polar amide functionalities.

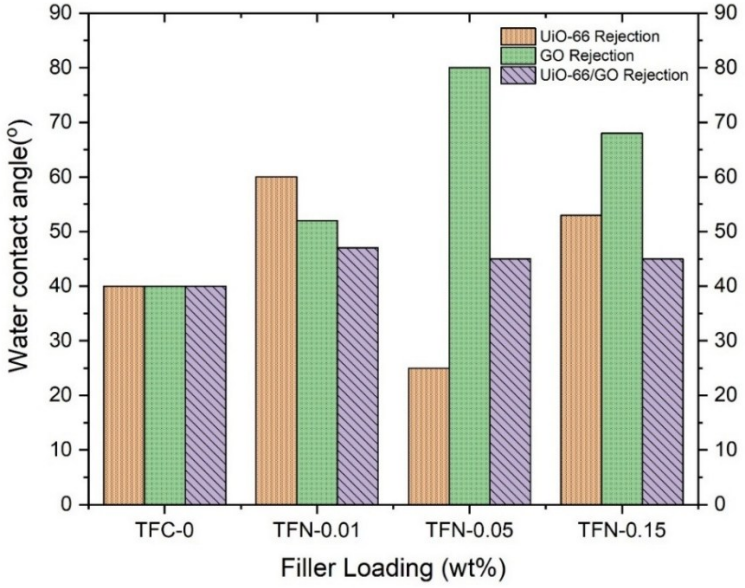

Figure 6. Static water contact angle (°) of pristine TFC and TFN membranes incorporating UiO-66, GO, and UiO-66/GO hybrid fillers at different loadings.

For UiO-66-based TFN membranes, the contact angle shows a strong dependence on filler loading. At low loading (0.01 wt%), the contact angle increases relative to the pristine membrane, suggesting partial exposure of hydrophobic aromatic moieties and surface roughness effects introduced during early filler incorporation. Upon increasing the UiO-66 loading to 0.05 wt%, a pronounced reduction in contact angle is observed, indicating enhanced surface hydrophilicity. This behavior can be attributed to the exposure of polar Zr–O clusters and carboxylate groups from the UiO-66 framework at the membrane surface. At the highest loading (0.15 wt%), the contact angle increases again, likely due to filler aggregation and surface heterogeneity, which partially masks hydrophilic sites and disrupts uniform surface chemistry.

GO-based TFN membranes display a contrasting trend, with contact angles generally increasing with filler loading. Despite the inherently hydrophilic nature of GO, excessive incorporation appears to promote surface roughness and possible restacking of GO sheets, leading to increased apparent hydrophobicity. This behavior aligns with the reduced water permeability observed for GO-based membranes and highlights that hydrophilicity alone does not guarantee enhanced membrane wettability when filler morphology induces unfavorable surface topology.

In contrast, TFN membranes incorporating UiO-66/GO composite fillers exhibit relatively stable and moderate contact angles across the investigated loading range. The composite membranes maintain contact angles close to those of the pristine polyamide membrane, indicating balanced surface wettability. This stability suggests that GO facilitates more uniform dispersion of UiO-66 within the polyamide layer, preventing excessive exposure of hydrophobic domains or aggregation-induced roughness. The controlled wettability of composite membranes is consistent with their improved permeability stability and enhanced Cr(VI) rejection performance.

Overall, the contact angle results demonstrate that surface wettability is governed not only by filler chemistry but also by filler dispersion and surface topology. The UiO-66/GO composite fillers provide a favorable balance between hydrophilicity and structural uniformity, reinforcing their role in achieving robust membrane performance without compromising surface properties.

3.3 Membrane Performance Evaluation

The effect of filler type and loading on the pure water permeability of TFN membranes is presented in Figure 7. The pristine TFC membrane (TFN 0) exhibits a baseline permeability of approximately 5 LMH bar^{-1}, which is consistent with the formation of a dense polyamide selective layer typical of nanofiltration membranes fabricated via interfacial polymerization. Upon incorporation of UiO-66 as a nanofiller, a pronounced enhancement in water permeability is observed at low and intermediate loadings. Specifically, the permeability increases sharply to ~14 LMH bar^{-1} at 0.01 wt% UiO-66 and reaches a maximum value of ~19 LMH bar^{-1} at 0.05 wt% loading, representing nearly a fourfold improvement compared to the pristine membrane. This enhancement can be attributed to the intrinsic microporosity and hydrophilic nature of UiO-66, which provide additional water transport pathways and promote facilitated water diffusion through the polyamide matrix. However, further increasing the UiO-66 loading to 0.15 wt% results in a noticeable decline in permeability. This non-monotonic behavior suggests that excessive filler incorporation leads to partial agglomeration and disruption of the polyamide network, which may increase transport resistance and hinder effective water pathways. Such an optimal loading phenomenon is commonly observed in thin-film nanocomposite membranes, where the balance between enhanced free volume and structural integrity governs transport performance.

In contrast, GO-based TFN membranes exhibit a markedly different trend. The incorporation of GO leads to a significant reduction in water permeability across all tested loadings, with permeability values decreasing to approximately 2 LMH bar^{-1}. This behavior can be attributed to the two-dimensional, sheet-like structure of GO, which tends to create tortuous transport pathways and may act as a barrier to water permeation when embedded within the polyamide layer. Despite the hydrophilic nature of GO, its planar geometry and potential stacking within the selective layer can outweigh its wettability benefits, resulting in suppressed water flux.

Notably, TFN membranes incorporating the UiO-66/GO composite display a more controlled and gradual permeability enhancement compared to single-filler systems. At low to moderate loadings, the permeability increases steadily, reaching approximately 12 LMH bar^{-1} at 0.15 wt% loading. This behavior suggests improved transport regulation resulting from the hybrid filler architecture. The porous UiO-66 structure provides additional pathways for water transport, while GO contributes to improved filler distribution and interfacial compatibility within the polyamide matrix. As a result, the composite-filled membranes maintain consistent permeability trends across the investigated loading range. This behavior is consistent with literature reports showing that hybrid nanofillers can improve transport continuity and regulate permeability without compromising membrane structural integrity.

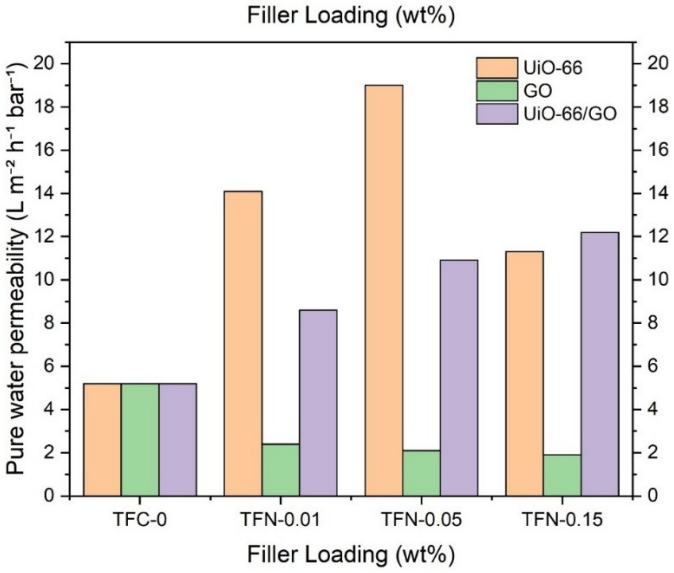

Figure 7. Pure water permeability of TFC and TFN membranes incorporating UiO-66, GO, and UiO-66/GO composite fillers at different loadings

The NaCl rejection performance of TFN membranes incorporating UiO-66, GO, and UiO-66/GO composite fillers at different loadings is summarized in Figure 8. The pristine TFC membrane exhibits a baseline NaCl rejection characteristic of a moderately dense polyamide nanofiltration layer, governed primarily by a combination of size exclusion and Donnan electrostatic effects. Upon incorporation of UiO-66, an initial decrease in NaCl rejection is observed at low filler loading, followed by a gradual recovery and enhancement at higher loadings. This behavior suggests that low concentrations of UiO-66 introduce localized disruptions or microvoids within the polyamide matrix, which temporarily weaken ionic selectivity. As the UiO-66 loading increases, the contribution of the MOF's intrinsic microporosity and surface charge becomes more pronounced, promoting enhanced ion–membrane interactions and restoring salt rejection through a more regulated transport pathway.

In contrast, GO-based TFN membranes display a monotonic decline in NaCl rejection with increasing filler loading. Although GO is rich in oxygen-containing functional groups, its two-dimensional lamellar structure can induce increased free volume heterogeneity and preferential water transport pathways when embedded in the polyamide layer. These structural effects reduce the effectiveness of electrostatic exclusion for monovalent ions such as Na^+ and Cl^-, leading to diminished salt rejection at higher GO loadings. The observed trend indicates that, in the absence of complementary porous fillers, excessive GO incorporation compromises ionic selectivity despite its hydrophilic nature.

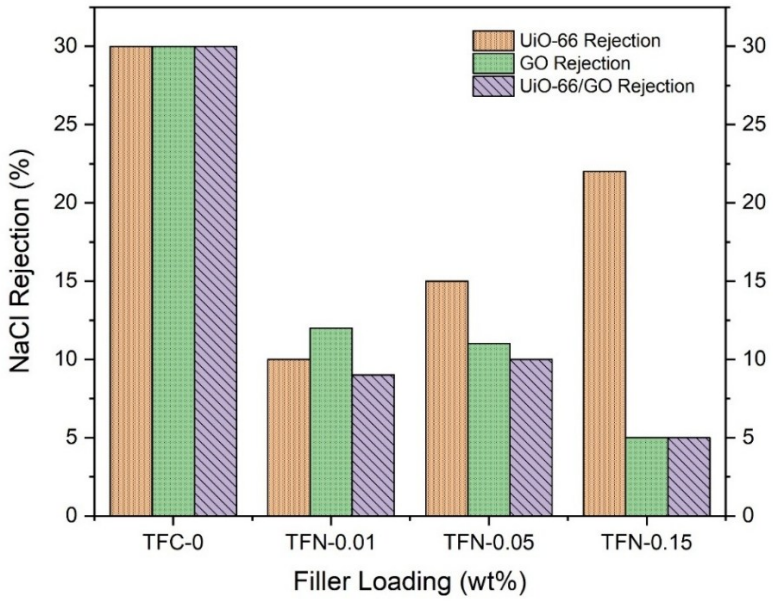

Figure 8. Effect of filler type and loading on NaCl rejection performance of TFN membranes incorporating UiO-66, GO, and UiO-66/GO composite fillers.

Notably, TFN membranes incorporating the UiO-66/GO composite exhibit a more balanced and controlled rejection profile across the investigated loading range. The composite-based membranes maintain moderate NaCl rejection without the sharp deterioration observed for GO-only systems or the pronounced non-monotonic behavior seen for UiO-66-only membranes. This behavior can be attributed to the synergistic integration of UiO-66 and GO, where UiO-66 provides rigid, porous domains that regulate ion transport, while GO enhances filler dispersion and interfacial compatibility within the polyamide layer. The resulting hybrid architecture mitigates excessive defect formation and preserves electrostatic selectivity, leading to a more stable rejection response.

Overall, the NaCl rejection results demonstrate that filler morphology and hybridization play a critical role in controlling ionic selectivity in TFN membranes. While single-component fillers introduce trade-offs between permeability enhancement and selectivity loss, the UiO-66/GO composite offers a more robust approach by balancing structural regulation and interfacial stability. This controlled rejection behavior is particularly advantageous for nanofiltration applications targeting selective

separation rather than complete desalination, and it highlights the potential of hybrid MOF-based fillers for advanced membrane design.

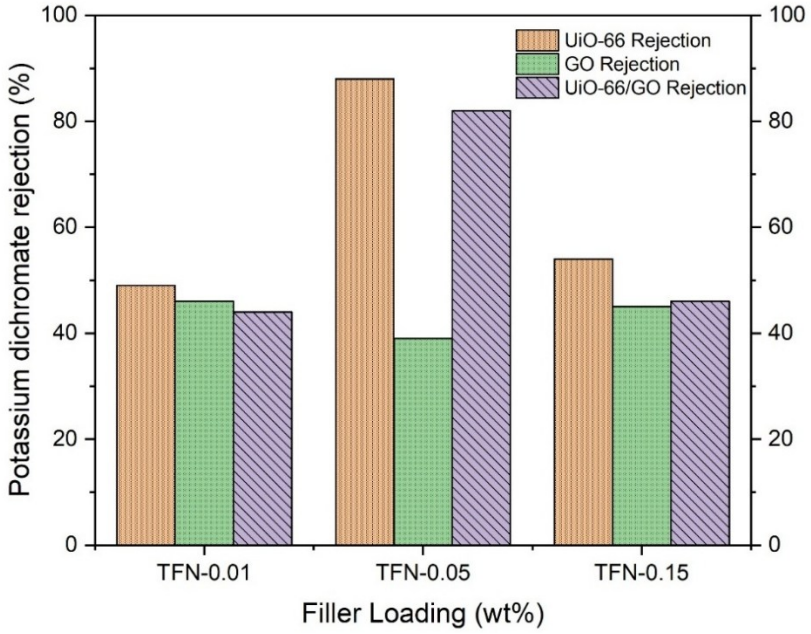

Figure 9. Potassium dichromate (Cr(VI)) rejection performance of TFN membranes incorporating UiO-66, GO, and UiO-66/GO composite fillers at different loadings

The rejection performance of potassium dichromate by all fabricated membranes, including the pristine PAN support, TFC membrane, and TFN membranes incorporating UiO-66, GO, and UiO-66/GO composite fillers at different loadings, is presented in Figure 9. A clear distinction in Cr(VI) rejection behavior is observed across the membrane architectures, reflecting differences in selective layer formation, surface charge characteristics, and filler–polymer interactions.

The pristine PAN support exhibits moderate Cr(VI) rejection, which can be attributed to its relatively large pore size and limited electrostatic exclusion capability. Upon formation of the polyamide selective layer, the TFC membrane demonstrates a noticeable improvement in Cr(VI) rejection, confirming the critical role of the dense polyamide layer in enabling nanofiltration behavior. This enhancement is primarily governed by Donnan electrostatic exclusion, as Cr(VI) exists predominantly as divalent oxyanions ($Cr_2O_7^{2-}$/CrO_4^{2-}) under the experimental conditions.

For UiO-66-based TFN membranes, Cr(VI) rejection shows a strong dependence on filler loading. At lower loadings, a slight reduction or plateau in rejection is observed, which can be attributed to localized perturbations in the polyamide matrix caused by filler incorporation. As the UiO-66 loading increases, Cr(VI) rejection improves substantially, reaching its highest values at intermediate to higher loadings. This enhancement is attributed to the combined effects of increased electrostatic repulsion and specific interactions between the zirconium-based UiO-66 framework and oxyanionic Cr(VI) species. The polar internal surface and coordinatively unsaturated Zr sites of UiO-66 are known to promote affinity toward anionic contaminants, thereby reinforcing charge-based exclusion.

In contrast, GO-based TFN membranes exhibit comparatively lower Cr(VI) rejection across the investigated loading range. Although GO contains abundant oxygen-containing functional groups, its two-dimensional lamellar structure can introduce non-selective transport pathways when embedded within the polyamide layer, partially weakening electrostatic exclusion. Increasing GO loading does not lead to a proportional improvement in Cr(VI) rejection, indicating that GO alone is insufficient to provide effective regulation of multivalent ion transport in the absence of rigid porous domains.

Notably, TFN membranes incorporating the UiO-66/GO composite display the most balanced and consistently high Cr(VI) rejection among all tested membranes. The composite-based membranes outperform both single-filler systems, particularly at optimized loadings, indicating a synergistic effect between UiO-66 and GO. In this hybrid architecture, UiO-66 provides structurally rigid, polar domains that promote electrostatic repulsion and affinity toward Cr(VI), while GO enhances filler dispersion and interfacial compatibility within the polyamide matrix. This synergy minimizes defect formation and strengthens Donnan exclusion, resulting in superior rejection of multivalent oxyanions.

Overall, the Cr(VI) rejection results clearly demonstrate that membrane performance is strongly influenced by filler chemistry and hybridization strategy. While single-component fillers introduce trade-offs between structural perturbation and selectivity enhancement, the UiO-66/GO composite offers a rational pathway to maximizing multivalent ion rejection. These findings highlight the potential of hybrid MOF-based TFN membranes for efficient removal of toxic chromium species from contaminated water streams.

The long-term stability of incorporated nanofillers is an important consideration for TFN membranes used in water treatment applications. In the present study, UiO-66, GO, and UiO-66/GO hybrid fillers were incorporated during interfacial polymerization and became physically confined within the highly crosslinked polyamide selective layer. This dense polymer network provides strong immobilization and limits filler mobility during filtration. In addition, the membranes demonstrated stable permeability and rejection performance under operating conditions, indicating preservation of selective layer integrity. Similar immobilization mechanisms have been widely reported in TFN membranes, where the polyamide matrix effectively retains nanofillers and maintains membrane stability during operation.

3.4 Practical Implications and Relevance for Water Treatment Applications

The findings of this study carry important practical implications for the development of next-generation nanofiltration membranes targeting heavy metal–contaminated water streams. The demonstrated ability of UiO-66/GO composite-based TFN membranes to simultaneously enhance multivalent ion rejection, maintain stable permeability, and preserve chemical integrity of the polyamide selective layer addresses several long-standing challenges associated with thin-film nanocomposite membrane design. In particular, the selective rejection of Cr(VI) species, which exist predominantly as toxic multivalent oxyanions in industrial effluents, highlights the suitability of the developed membranes for applications such as electroplating wastewater treatment, leather tanning effluents, and mining-impacted water sources.

From a materials perspective, the use of low filler loadings (<0.15 wt%) is especially relevant for scalable membrane fabrication, as it minimizes risks associated with filler agglomeration, excessive viscosity changes in the organic phase, and defect formation during interfacial polymerization. The retention of polyamide chemistry and the absence of covalent disruption indicate that the proposed hybrid filler strategy can be readily integrated into existing industrial membrane manufacturing workflows without requiring major process modifications. This compatibility is a critical consideration for commercial adoption, where reliability and reproducibility often outweigh marginal performance gains.

Moreover, the synergistic role of UiO-66 and GO in regulating ion transport pathways underscores the importance of hybrid filler architectures over single-component nanomaterials. While UiO-66 provides rigid, polar domains conducive to electrostatic exclusion and affinity toward oxyanionic contaminants, GO enhances filler dispersion and interfacial compatibility, mitigating the performance instability typically observed at higher filler loadings. This balance enables a tunable membrane design strategy, allowing performance optimization based on target contaminants rather than relying on one-size-fits-all solutions.

The observed preferential rejection of Cr(VI) relative to monovalent salts positions these membranes within the functional regime of nanofiltration rather than desalination, making them particularly attractive for selective separation processes where complete salt removal is neither necessary nor desirable. Such selectivity can translate into lower operating pressures, reduced energy consumption, and improved process economics when treating industrial wastewaters with complex ionic compositions. Overall, this work demonstrates a rational pathway toward the design of TFN membranes that combine structural stability, selective ion rejection, and scalable fabrication. The insights gained from correlating filler chemistry, dispersion, and membrane performance

provide a framework that can be extended to other MOF-based hybrid systems and target contaminants, thereby contributing to the broader advancement of membrane technologies for sustainable water treatment.

From a scalability perspective, the incorporation of UiO-66, GO, and hybrid fillers was performed at low concentrations, which minimizes changes in organic phase viscosity and allows uniform dispersion during interfacial polymerization. The fabrication method employed in this study follows conventional interfacial polymerization protocols widely used in industrial thin-film composite membrane manufacturing. This ensures compatibility with existing large-scale production processes. However, at higher filler loadings, careful control of dispersion and solution properties may be required to maintain uniform selective layer formation. These considerations are consistent with established TFN membrane fabrication practices and suggest that the hybrid filler strategy presented in this work is compatible with scalable membrane production.

4. Conclusions

In this study, thin film nanocomposite nanofiltration membranes incorporating UiO-66, graphene oxide (GO), and UiO-66/GO hybrid fillers were successfully fabricated via interfacial polymerization and systematically evaluated for water treatment applications. Structural and chemical characterization confirmed that the crystalline integrity of UiO-66 and the chemical structure of the polyamide selective layer were preserved after filler incorporation, while hybridization with GO improved filler dispersion and interfacial compatibility. Membrane performance results revealed that filler morphology and hybridization play a decisive role in governing transport and selectivity. UiO-66-based TFN membranes exhibited substantial enhancement in water permeability at optimal loadings, whereas GO-only membranes suffered from permeability and selectivity trade-offs due to lamellar transport resistance. Notably, UiO-66/GO composite-based membranes demonstrated a balanced and stable performance, combining controlled permeability with enhanced rejection of multivalent Cr(VI) species. The preferential rejection of potassium dichromate relative to NaCl confirms that separation is dominated by Donnan electrostatic exclusion reinforced by filler-induced regulation of transport pathways. Contact angle and surface analyses further showed that hybrid filler incorporation enables tunable surface wettability without compromising membrane integrity, contributing to stable performance across a range of filler loadings. Importantly, the use of low filler concentrations and the retention of conventional interfacial polymerization chemistry highlight the scalability and practical relevance of the proposed membrane design. Overall, this work establishes UiO-66/GO hybrid fillers as an effective strategy for overcoming the limitations of single-component TFN membranes and provides a rational framework for designing next-generation nanofiltration membranes targeting selective removal of toxic multivalent contaminants from water.

Declaration of Generative AI

During the preparation of this work, the authors used ChatGPT to refine writing and improve readability. The authors have reviewed and edited the AI-generated content as necessary and take full responsibility for the contents of this publication.

Data Availability Statement

The data that support the findings of this study are available from the corresponding author upon reasonable request.

Funding Statement

This research did not receive any specific grant from funding agencies in the public, commercial, or not-for-profit sectors.

Author Contributions

Muhammad Ammar Farooq: Conceptualization, Methodology, Writing – original draft. Noaman Ul Haq: Supervision, Conceptualization, Project administration, Reviewing and Editing. Ghulam Muhammad: Methodology, Validation, Reviewing and Editing. Hira Naveed: Data curation, Reviewing and Editing.

References

[1] Sharma, S., Bhattacharya, A. "Drinking water contamination and treatment techniques". *Applied Water Science*, *7*(3), pp. 1043–1067. 2017. DOI:10.1007/s13201-016-0455-7

[2] Warsinger, D. M., Chakraborty, S., Tow, E. W., Plumlee, M. H., Bellona, C., Loutatidou, S., … Lienhard, J. H. "A review of polymeric membranes and processes for potable water reuse". *Progress in Polymer Science*, *81*, pp. 209–237. 2018. DOI:10.1016/J.PROGPOLYMSCI.2018.01.004

[3] Barakat, M. A. "New trends in removing heavy metals from industrial wastewater". *Arabian Journal of Chemistry*, *4*(4), pp. 361–377. 2011. DOI:10.1016/J.ARABJC.2010.07.019

[4] Mohan, D., Pittman, C. U. "Activated carbons and low cost adsorbents for remediation of tri- and hexavalent chromium from water". *Journal of Hazardous Materials*, *137*(2), pp. 762–811. 2006. DOI:10.1016/J.JHAZMAT.2006.06.060

[5] Miretzky, P., Cirelli, A. F. "Cr(VI) and Cr(III) removal from aqueous solution by raw and modified lignocellulosic materials: A review". *Journal of Hazardous Materials*, *180*(1–3), pp. 1–19. 2010. DOI:10.1016/J.JHAZMAT.2010.04.060

[6] Owlad, M., Aroua, M. K., Daud, W. A. W., Baroutian, S. "Removal of Hexavalent Chromium-Contaminated Water and Wastewater: A Review". *Water, Air, and Soil Pollution*, *200*(1), pp. 59–77. 2009. DOI:10.1007/s11270-008-9893-7

[7] Fu, F., Wang, Q. "Removal of heavy metal ions from wastewaters: A review". *Journal of Environmental Management*, *92*(3), pp. 407–418. 2011. DOI:10.1016/J.JENVMAN.2010.11.011

[8] Babel, S., Kurniawan, T. A. "Low-cost adsorbents for heavy metals uptake from contaminated water: a review". *Journal of Hazardous Materials*, *97*(1–3), pp. 219–243. 2003. DOI:10.1016/S0304-3894(02)00263-7

[9] de Clippel, F., Khan, A. L., Cano-Odena, A., Dusselier, M., Vanherck, K., Peng, L., … Sels, B. F. "CO2 reverse selective mixed matrix membranes for H2 purification by incorporation of carbon–silica fillers". *Journal of Materials Chemistry A*, *1*(3), pp. 945–953. 2013. DOI:10.1039/C2TA00098A

[10] Ur Rehman, R., Rafiq, S., Muhammad, N., Khan, A. L., Ur Rehman, A., TingTing, L., … Gu, X. "Development of ethanolamine-based ionic liquid membranes for efficient CO2/CH4 separation". *Journal of Applied Polymer Science*, *134*(44), pp. 45395. 2017. DOI:https://doi.org/10.1002/app.45395

[11] Ishaq, M., Gilani, M. A., Afzal, Z. M., Bilad, M. R., Nizami, A.-S., Rehan, M., … Khan, A. L. "Novel Poly Deep Eutectic Solvents Based Supported Liquid Membranes for CO2 Capture". *Frontiers in Energy Research*, *Volume 8-2020*. 2020. Retrieved from https://www.frontiersin.org/journals/energy-research/articles/10.3389/fenrg.2020.595041

[12] Kiran, A., Anjum, T., Khan, A. L., AlMohamadi, H., Kiran, S., Gilani, M. A., … Yasin, M. "Enhancing water purification efficiency with zirconium-mercaptosuccinic acid metal-organic framework integrated mixed matrix membranes: Synthesis, comprehensive characterization, and performance insights". *Chemical Engineering Research and Design*, *211*, pp. 9–20. 2024. DOI:10.1016/J.CHERD.2024.09.021

[13] Sahar, T., Tamime, R., Usman, M., AlMohamadi, H., Nawaz, R., Anjum, T., Khan, A. L. "Tailoring thin film composite membranes for enhanced removal of heavy metals from water". *Journal of Applied Polymer Science*, *141*(48), pp. e56295. 2024. DOI:https://doi.org/10.1002/app.56295

[14] Figoli, A., Marino, T., Simone, S., Di Nicolò, E., Li, X.-M., He, T., … Drioli, E. "Towards non-toxic solvents for membrane preparation: a review". *Green Chemistry*, *16*(9), pp. 4034–4059. 2014. DOI:10.1039/C4GC00613E

[15] Elimelech, M., Phillip, W. A. "The Future of Seawater Desalination: Energy, Technology, and the Environment". *Science*, *333*(6043), pp. 712–717. 2011. DOI:10.1126/science.1200488

[16] Strathmann, H., Kock, K. "The formation mechanism of phase inversion membranes". *Desalination*, *21*(3), pp. 241–255. 1977. DOI:10.1016/S0011-9164(00)88244-2

[17] LOEB, S., SOURIRAJAN, S. "Sea Water Demineralization by Means of an Osmotic Membrane". In *Saline Water*

Conversion—II (Vol. 38, pp. 117-132 SE–9). AMERICAN CHEMICAL SOCIETY. 1963. DOI:doi:10.1021/ba-1963-0038.ch009

[18] Caro, J., Noack, M. "Zeolite membranes – Recent developments and progress". *Microporous and Mesoporous Materials*, *115*(3), pp. 215–233. 2008. DOI:10.1016/J.MICROMESO.2008.03.008

[19] Julbe, A., Rouessac, V., Durand, J., Ayral, A. "New approaches in the design of ceramic and hybrid membranes". *Journal of Membrane Science*, *316*(1–2), pp. 176–185. 2008. DOI:10.1016/J.MEMSCI.2007.08.055

[20] Wanjiya, M., Zhang, J. C., Wu, B., Yin, M. J., An, Q. F. "Nanofiltration membranes for sustainable removal of heavy metal ions from polluted water: A review and future perspective". *Desalination*, *578*, pp. 117441. 2024. DOI:10.1016/J.DESAL.2024.117441

[21] Liu, Y., Zhu, J., Chi, M. S., Eygen, G. Van, Guan, K., Matsuyama, H. "Comprehensive review of nanofiltration membranes for efficient resource recovery from textile wastewater". *Chemical Engineering Journal*, *506*, pp. 160132. 2025. DOI:10.1016/J.CEJ.2025.160132

[22] Wang, B., Li, T., Li, T., Cheng, C., Zhang, K., Han, G., … Wang, L. "Preparation and application of metal–organic framework-based mixed matrix membranes for water treatment". *Desalination and Water Treatment*, *286*, pp. 29–39. 2023. DOI:10.5004/DWT.2023.29319

[23] Denny, M. S., Moreton, J. C., Benz, L., Cohen, S. M. "Metal–organic frameworks for membrane-based separations". *Nature Reviews Materials*, *1*(12), pp. 16078. 2016. DOI:10.1038/natrevmats.2016.78

[24] Bilal, A., Yasin, M., Akhtar, F. H., Gilani, M. A., Almohamadi, H., Younas, M., … Khan, A. L. "Enhancing Water Purification by Integrating Titanium Dioxide Nanotubes into Polyethersulfone Membranes for Improved Hydrophilicity and Anti-Fouling Performance". *Membranes*. 2024. DOI:10.3390/membranes14050116

[25] Barzegar, B., Habibi, R., Aghdasinia, H. "Mixed matrix membranes incorporating waste tire-derived activated carbon decorated with zeolite imidazolate frameworks into polyether sulfone for enhanced permeability, antifouling properties, and wastewater applications". *Chemical Engineering Journal*, *508*, pp. 161032. 2025. DOI:10.1016/J.CEJ.2025.161032

[26] Hadi, G. J., Ariana, M. A., Alibak, A. H., Hassanvand, A. "Evaluation and comparison of UiO66 and its functionalized variants for the removal of Cu (II) ions from wastewater". *Polymer*, *315*, pp. 127760. 2024. DOI:10.1016/J.POLYMER.2024.127760

[27] Rego, R. M., Kurkuri, M. D., Kigga, M. "A comprehensive review on water remediation using UiO-66 MOFs and their derivatives". *Chemosphere*, *302*, pp. 134845. 2022. DOI:10.1016/J.CHEMOSPHERE.2022.134845

[28] Ji, S., Abdel-Fattah, T. M. "Advancing Arsenic Water Treatment Using UiO-66 and Its Functionalized Metal–Organic Framework Analogs". *Nanomaterials*. 2025. DOI:10.3390/nano15211621

[29] Yuan, F., Yan, D., Song, S., Zhang, J., Yang, Y., Chen, Z., … Sun, Y. "Removal of heavy metals from water by adsorption on metal organic frameworks: Research progress and mechanistic analysis in the last decade". *Chemical Engineering Journal*, *506*, pp. 160063. 2025. DOI:10.1016/J.CEJ.2025.160063

[30] Abioye, S. O., Majooni, Y., Moayedi, M., Rezvani, H., Kapadia, M., Yousefi, N. "Graphene-based nanomaterials for the removal of emerging contaminants of concern from water and their potential adaptation for point-of-use applications". *Chemosphere*, *355*, pp. 141728. 2024. DOI:10.1016/J.CHEMOSPHERE.2024.141728

[31] Elzubair, A., Uchôa, L. R., Prado da Silva, M. H. "Production and characterization of graphene oxide/polymer support composite membranes for water desalination and purification". *Desalination and Water Treatment*, *317*, pp. 100012. 2024. DOI:10.1016/J.DWT.2024.100012

[32] Han, Y., Xu, Z., Gao, C. "Ultrathin Graphene Nanofiltration Membrane for Water Purification". *Advanced Functional Materials*, *23*(29), pp. 3693–3700. 2013. DOI:https://doi.org/10.1002/adfm.201202601

[33] Mukherjee, R., Bhunia, P., De, S. "Impact of graphene oxide on removal of heavy metals using mixed matrix membrane". *Chemical Engineering Journal*, *292*, pp. 284–297. 2016. DOI:10.1016/J.CEJ.2016.02.015

[34] Iqbal, Z., Shamair, Z., Usman, M., Gilani, M. A., Yasin, M., Saqib, S., Khan, A. L. "One pot synthesis of UiO-66@IL composite for fabrication of CO2 selective mixed matrix membranes". *Chemosphere*, *303*, pp. 135122. 2022. DOI:10.1016/J.CHEMOSPHERE.2022.135122